

Sensorless Control of Dual Star Induction Machine

Boumediene Benabdallah Sereir^{*1}, Farid Saadaoui² and Ahmed Tahour³

¹LSTE Laboratory, Department of Electrical Engineering/ Faculty of Sciences and technology, M.S Mascara University, Algeria

<https://orcid.org/0009-0008-8448-655X>

² Department of Electrical Engineering/ Faculty of Sciences and technology, M.S Mascara University, Algeria

³ Department of Electrical Engineering, Ecole Supérieur en Sciences appliquées de Tlemcen (ESSA), Algeria

[*benabdallahboumediene@yahoo.fr](mailto:benabdallahboumediene@yahoo.fr)

(Received: 12 February 2025, Accepted: 17 February 2025)

(2nd International Conference on Recent and Innovative Results in Engineering and Technology ICRIRET, February 11-12, 2025)

ATIF/REFERENCE: Sereir, B. B., Saadaoui, F. & Tahour, A. (2025). Sensorless Control of Dual Star Induction Machine. *International Journal of Advanced Natural Sciences and Engineering Researches*, 9(2), 252-260.

Abstract – This paper is devoted to the control without mechanical sensor of a dual star induction machine (DSIM) supplied by two voltage inverters. For this we will first present the dynamic model of the machine based on the Park transformation. To improve the decoupling between flux and torque, a control technique known as direct torque control (DTC) was applied. Then, we present the synthesis of a robust technique based on the sliding mode for speed regulation. To eliminate the mechanical sensor and reduce the cost of the drive system, we have presented a MRAS observer.

Keywords – Dual Star Induction Machine (DSIM) —Sliding Mode Control—Direct Torque Control (DTC) —MRAS Observer.

I. INTRODUCTION

Multiphase machines are advantageous than conventional machines. Among these advantages we can cite reliability, power segmentation by increasing the number of phases, power is automatically increased and torque ripples and rotor losses are minimized.

MASDE's direct torque control (DTC) has been introduced to improve system performance and to be well controlled a robust tuning technique has been applied: the sliding mode.

The sliding mode control (SMC) has been used very successful in recent years, this is due to its simplicity of implementation and its robustness with regard to the uncertainties of the system and to the external disturbances affecting the process. (The typical sliding mode control design consists of two phases: sliding phase design and reaching phase design. In this case SMC consists of two parts: the first allowing the approach until reaching the surface, the second allowing the maintenance of the slide along this surface. The control without a speed sensor is described using the sliding mode control. Finally, we simulate the operation in real time of the inverter-MADE-control assembly.

The results obtained with the proposed (SMC) algorithm, the MRAS observer as well as the robustness tests with respect to disturbances are analyzed.

II. MODELISATION OF DSIM

The dual star induction machine, in the conventional configuration, has two identical three-phase windings.

The two stars share the same stator and are offset by an electrical angle of α° . These windings have the same number of poles and are fed at the same frequency. The structure of the rotor remains identical to a three-phase machine ([1], [2]).

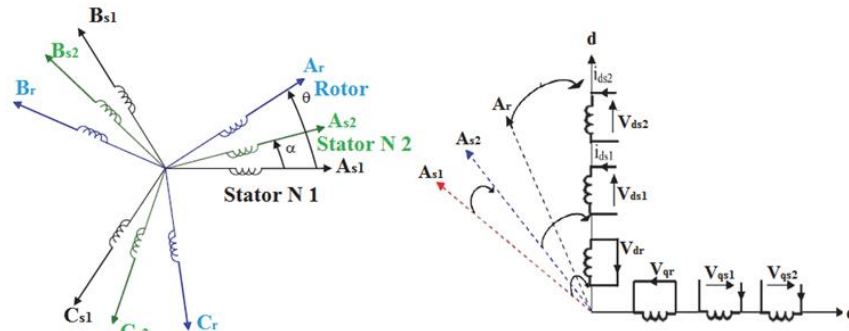


Fig. 1 PARK model of DSIM

A. Equation of voltage [3]

The voltage of stator and rotor are:

$$\begin{cases} v_{ds1,2} = R_{s1,2}i_{ds1,2} + \frac{d}{dt}\phi_{ds1,2} - \omega_s\phi_{qs1,2} \\ v_{qs1,2} = R_{s1,2}i_{qs1,2} + \frac{d}{dt}\phi_{qs1,2} - \omega_s\phi_{ds1,2} \\ 0 = R_r i_{dr} + \frac{d}{dt}\phi_{dr} - (\omega_s - \omega_r)\phi_{qr} \\ 0 = R_r i_{qr} + \frac{d}{dt}\phi_{qr} - (\omega_s - \omega_r)\phi_{dr} \end{cases} \quad (1)$$

B. Equation of flux linkage

The flux linkage in each phase is:

$$\begin{cases} \phi_{ds1} = L_{s1}i_{ds1} + L_m(i_{ds1} + i_{ds2} + i_{dr}) \\ \phi_{qs1} = L_{s1}i_{qs1} + L_m(i_{qs1} + i_{qs2} + i_{qr}) \\ \phi_{ds2} = L_{s2}i_{ds2} + L_m(i_{ds1} + i_{ds2} + i_{dr}) \\ \phi_{qs2} = L_{s2}i_{qs2} + L_m(i_{qs1} + i_{qs2} + i_{qr}) \\ \phi_{dr} = L_r i_{dr} + L_m(i_{ds1} + i_{ds2} + i_{dr}) \\ \phi_{qr} = L_r i_{qr} + L_m(i_{qs1} + i_{qs2} + i_{qr}) \end{cases} \quad (2)$$

C. The mechanical equation

The motion equation is:

$$\begin{cases} J \frac{d}{dt}\Omega_m = C_{em} - C_r - K_f\Omega_m \\ C_{em} = p \frac{L_m}{L_m + L_r} [(i_{qs1} + i_{qs2})\phi_{dr} - (i_{ds1} + i_{ds2})\phi_{qr}] \end{cases} \quad (3)$$

III. DESCRIPTION OF THE SYSTEM

FIG. 2 represents the schematic diagram of the control of the system studied. The sliding mode control block contains the speed controller. DTC contains in the first, the forward torque regulator and the second is the flux regulator. The speed of the machine is estimated by a MRAS observer.

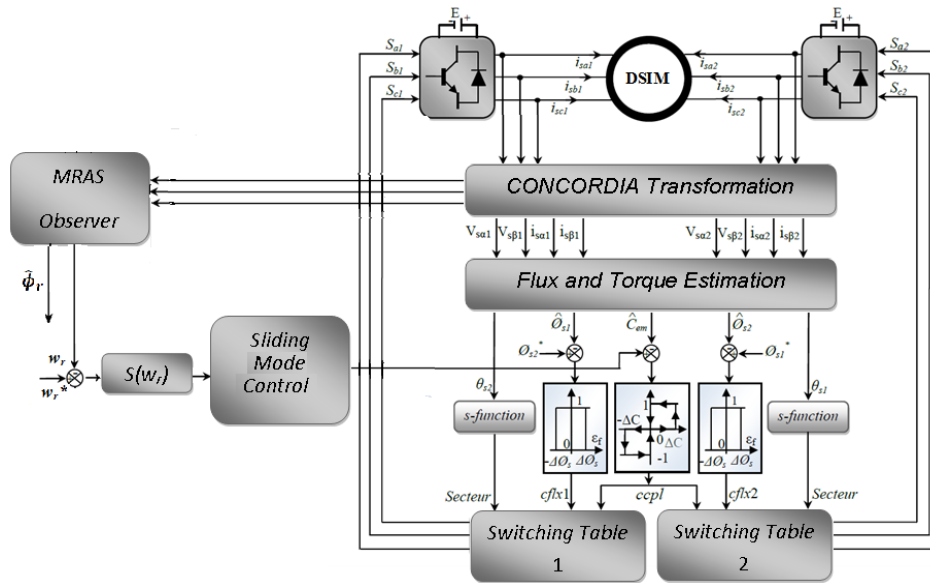


Fig. 2 Block diagram of Direct Torque Control for DSIM

IV. DIRECT TORQUE CONTROL

Direct torque control (DTC) consists in directly controlling the closing or opening of the inverter switches from the pre-calculated values of the stator flux and the torque. Changes in switch states are linked to changes in the electromagnetic states of the motor. They are no longer controlled from the voltage and frequency instructions given to the close control of an inverter with pulse width modulation [4].

The reference values of flux (ϕ_s^*) and torque (T_{em}^*) are compared to their actual values and the resultant errors are fed into a two level hysteresis comparator for the flux and three level hysteresis comparator for the torque, who allows controlling the motor in the two directions of rotation (Fig.3).

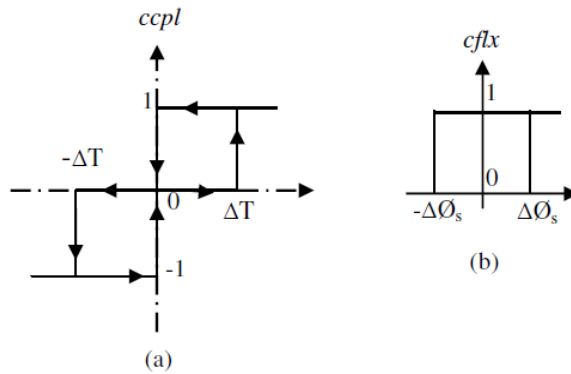


Fig. 3 Block Hysteresis comparator, (a): three level hysteresis comparator for the torque, (b): two level hysteresis comparator for the flux

The stator flux expression is given by [5]:

$$\overline{\phi}_s(t) = \int_0^t (\overline{V}_s - R_s \overline{I}_s) dt \tag{4}$$

Between two switchings of the inverter switches, the selected voltage vector is always the same.

$$\overline{\phi}_s(t) = \overline{\phi}_{s_0} + \overline{V}_s t - \int_0^t (R_s \overline{I}_s) dt \tag{5}$$

Neglecting the resistive term [5]:

$$\overline{\phi}_s(t) = \overline{V}_s + \overline{\phi}_{s_0} \tag{6}$$

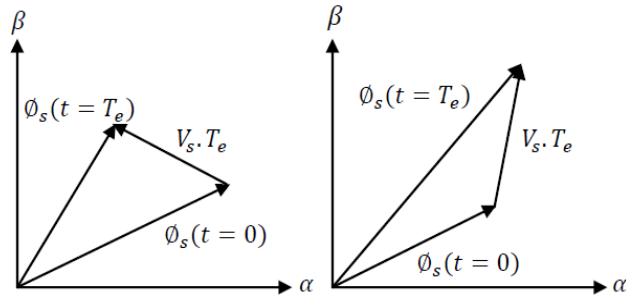


Fig. 4 Application of a voltage vector stator

The stator flux and the rotor flux can be put in the following complex form:

$$\begin{cases} \bar{\phi}_s = [\phi_s, \theta_s] = \phi_s \cdot e^{j\theta_s} \\ \bar{\phi}_r = [\phi_r, \theta_r] = \phi_r \cdot e^{j\theta_r} \end{cases} \quad (7)$$

$\bar{\phi}_s$: is the stator flux vector

$\bar{\phi}_r$: is the rotor flux vector

The torque can be expressed as follows [6]:

$$C_{em} = K_c \|\bar{\phi}_s\| \cdot \|\bar{\phi}_r\| \sin(\gamma_0) \quad (8)$$

With :

$$K_c = \frac{3 p M_{sr}}{2(\sigma L_s \cdot L_r)}$$

$$\gamma_0 = \theta_{s0} - \theta_{r0}$$

Or

K_c : constant depending on the parameters of the machine.

γ_0 : Angle between the two vectors stator and rotor flux.

By considering the flux vector ϕ_s in the stator frame of reference divided into six sectors, the vectors: V_1 , V_6 and V_2 can be selected to increase its amplitude.

Conversely, the decrease of ϕ_s can be obtained by the selection of vectors: V_3 , V_5 and V_4 , the zero vector hardly affects the stator flux vector, except for a small attenuation due to stator voltage drop [7].

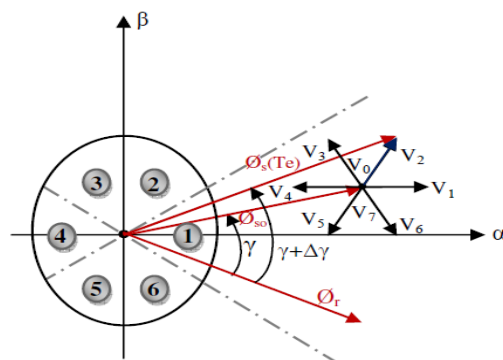


Fig. 5 Voltage vector selection

The tables below summarize, in general, the active voltage sequences to be applied to increase or decrease the stator flux modulus and the torque electromagnetic depending on the sector.

Table 1. switching table of flux

	N=1	N=2	N=3	N=4	N=5	N=6
$\phi_s \uparrow$	V_6, V_1, V_2	V_1, V_2, V_3	V_2, V_3, V_4	V_3, V_4, V_5	V_4, V_5, V_6	V_5, V_6, V_1
$\phi_s \downarrow$	V_3, V_4, V_5	V_4, V_5, V_6	V_5, V_6, V_1	V_6, V_1, V_2	V_1, V_2, V_3	V_2, V_3, V_4

Table 2. switching table of Torque

	N=1	N=2	N=3	N=4	N=5	N=6
$C_{em} \uparrow$	V_2, V_3	V_3, V_4	V_4, V_5	V_5, V_6	V_6, V_1	V_1, V_2
$C_{em} \downarrow$	V_3, V_4	V_4, V_5	V_5, V_6	V_6, V_1	V_1, V_2	V_2, V_3

Finally, the comparison of the two switching tables allows the final synthesis of a single switching table, the latter can be divided into two other tables, the first with zero voltage vectors and the second with active voltage vectors (not zero):

Table 3. Switching table with zero voltage vectors

Sectors			1	2	3	4	5	6	
$cflx$	0	$ccpl$	1	V_3	V_4	V_5	V_6	V_1	V_2
			0	V_0	V_7	V_0	V_7	V_0	V_7
			-1	V_5	V_6	V_1	V_2	V_3	V_4
$cflx$	1	$ccpl$	1	V_2	V_3	V_4	V_5	V_6	V_1
			0	V_7	V_0	V_7	V_0	V_7	V_0
			-1	V_6	V_1	V_2	V_3	V_4	V_5

V. SLIDING MODE CONTROL

A. Sliding mode Principe

The variable structure control has appeared since the beginning of the 60c, thanks to the theoretical results of the mathematician A.F. Philipov. It is a type of nonlinear control based on the use of a discontinuous term. Because of the problems of chattering and realization, the variable structure control had to wait until the end of the Seventies to see its reappearance together with important advances in electronics and computing. Fig 6 presents the phase plane trajectory of a system being stabilized by a sliding mode controller ([8], [9]).

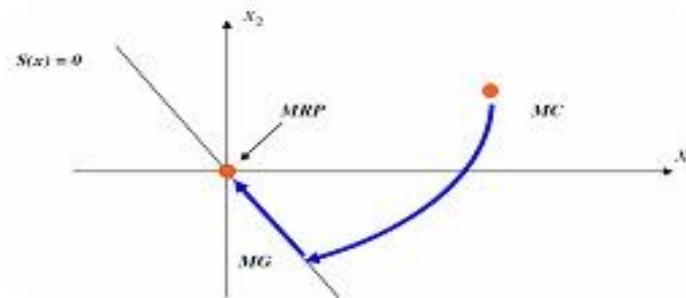


Fig. 6 Phase plane trajectory

The two components of the control are then defined by :

$$u + u_{eq} + u_f \quad \text{and} \quad u_f = K \cdot \text{sign}(s(x)) \quad K > 0 \quad (9)$$

B. Speed Control

The surface of speed is defined by:

$$S(\Omega) = \Omega^* - \Omega \quad (10)$$

$$\dot{S}(\Omega) = \dot{\Omega}^* - \dot{\Omega} \quad (11)$$

From the mechanical equation we have:

$$\dot{\Omega} = \frac{d\Omega}{dt} = \frac{1}{J} (C_{em} - C_f - C_r) \quad (12)$$

$$\dot{\Omega} = \frac{d\Omega}{dt} = \frac{1}{J} (C_{em} - K_f \Omega - C_r) \quad (13)$$

$$\dot{S}(\Omega) = \dot{\Omega}^* - \frac{C_{em}}{J} + \frac{K_f}{J} \Omega + \frac{1}{J} C_r \quad (14)$$

We replace C_{em} by C_{em}^* including:

$$C_{em}^* = C_{em}^{eq} + C_{em} \quad (15)$$

we obtain:

$$\dot{S}(\Omega) = \dot{\Omega}^* - \frac{C_{em}^{eq}}{J} - \frac{C_{em}^n}{J} + \frac{K_f \cdot \Omega}{J} + \frac{C_r}{J} \quad (16)$$

In permanent regime, the surface:

$$S(\Omega) = 0 ; \dot{S}(\Omega) = 0 ; C_{em}^n = 0 \quad (17)$$

So we will have:

$$C_{em}^{eq} = J\dot{\Omega}^* + K_f \cdot \Omega + C_r \quad (18)$$

we have : $\Omega = \frac{\omega_r}{p}$

$$C_{em}^{eq} = \frac{J}{p} \cdot \dot{\omega}_r^* + C_r \quad (19)$$

$$C_{em}^n = K \cdot \text{Sign}(S(\omega_r)) \quad (20)$$

VI. SPEED OBSERVER

The adaptive system using a reference model (MRAS) is composed of two flux estimators. The first, which does not introduce speed, is called the reference model (usually it is a current model). The second is called the adjustable model (usually a voltage model) (Figure 7). The error, produced by the offset between the outputs of two estimators, controls an adaptation algorithm that generates the estimated speed $\hat{\omega}_r$ [10]. The latter is applied to the adjustable model. For the dual star induction motor, the adaptive model of observer is described by equation (21):

$$\begin{cases} \frac{d\hat{\phi}_{rai}}{dt} = \frac{L_m}{T_r} (i_{\alpha s1} + i_{\beta s1}) - \frac{1}{T_r} \hat{\phi}_{rai} - \omega_r \hat{\phi}_{r\beta i} \\ \frac{d\hat{\phi}_{r\beta i}}{dt} = \frac{L_m}{T_r} (i_{\alpha s1} + i_{\beta s1}) - \frac{1}{T_r} \hat{\phi}_{r\beta i} - \omega_r \hat{\phi}_{rai} \end{cases} \quad (21)$$

And the reference model is given by equation (22)

$$\begin{cases} \frac{d\hat{\phi}_{rav}}{dt} = \frac{L_r + L_m}{T_r} (v_{\alpha s1} - R_s i_{\alpha s1} - \sigma(L_r + L_m) \frac{di_{\alpha s1}}{dt} - \frac{L_m L_r}{L_m + L_r} \frac{di_{\alpha s2}}{dt}) \\ \frac{d\hat{\phi}_{r\beta v}}{dt} = \frac{L_r + L_m}{L_m} (v_{\beta s1} - R_s i_{\beta s1} - \sigma(L_r + L_m) \frac{di_{\beta s1}}{dt} - \frac{L_m L_r}{L_m + L_r} \frac{di_{\alpha s2}}{dt}) \end{cases} \quad (22)$$

The error for the corrector is calculated according to the cross product [11] [12]

$$\varepsilon = \hat{\phi}_{ari} \cdot \phi_{\beta rv} - \hat{\phi}_{arv} \cdot \phi_{r\beta i} \quad (23)$$

The difference between the outputs of the two flux estimators is used to correct the speed estimate [13]

The law of adaptation is given by the following expression:

$$\hat{\omega}_r = \varepsilon \left(k_p + \frac{k_i}{s} \right) \quad (24)$$

This translates simply by the use of a PI regulator as a mechanism of adaptation

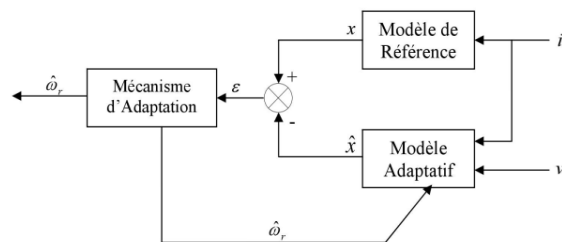


Fig. 7 MRAS Structure

VII. SIMULATION

To show the sliding mode, DTC controller and MRAS observer performances we have simulated the system described in figure 2.

In order to test the robustness of the control used, we present the simulation results of the DTC control with regulator (sliding mode) with and without mechanical sensors of the MASDE, using the MRAS observer. Simulation results for a cycle speed of 300 (rad /s) and reversal of the direction of rotation, with application of a load torque of 14 Nm are given by figure (8) and figure (9).

Figure 8 shows the robustness tests performed by the DTC-SM with mechanical sensor and application of the load $C_r = 14 \text{ N.m}$ to the instance $t_1 = 2\text{s}$ and its elimination at $t_2 = 3\text{s}$.

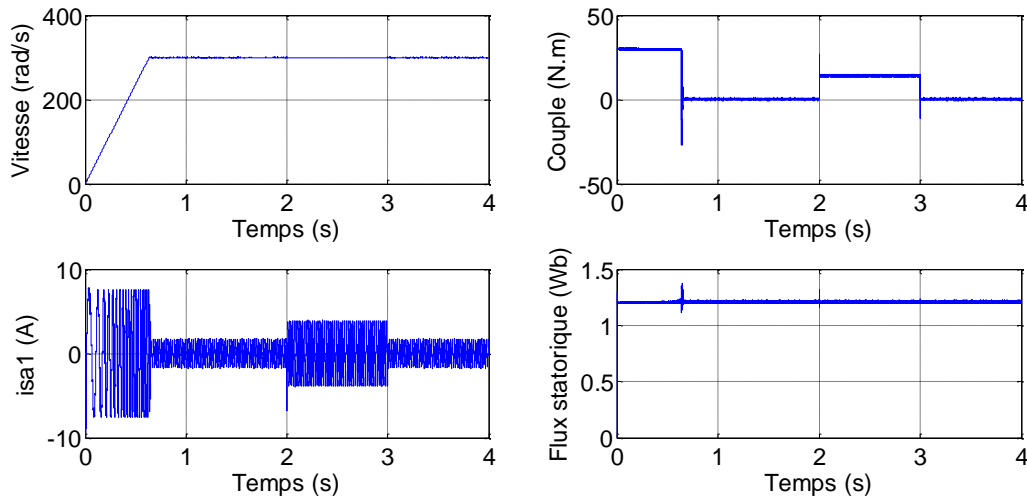


Fig. 8 Direct Torquecontrol of the MASDE with a speed regulator by sliding mode by applying a load torque $C_r = 14 \text{ N.m}$ between 2s and 3s

Figure 9 illustrates the performance of the control without a mechanical sensor using the MRAS observer. The results of this figures show the high performance of the speed observer for different speed variations.

From using the sliding mode technique, DTC and MRAS observer we have reached high performances in control and observation

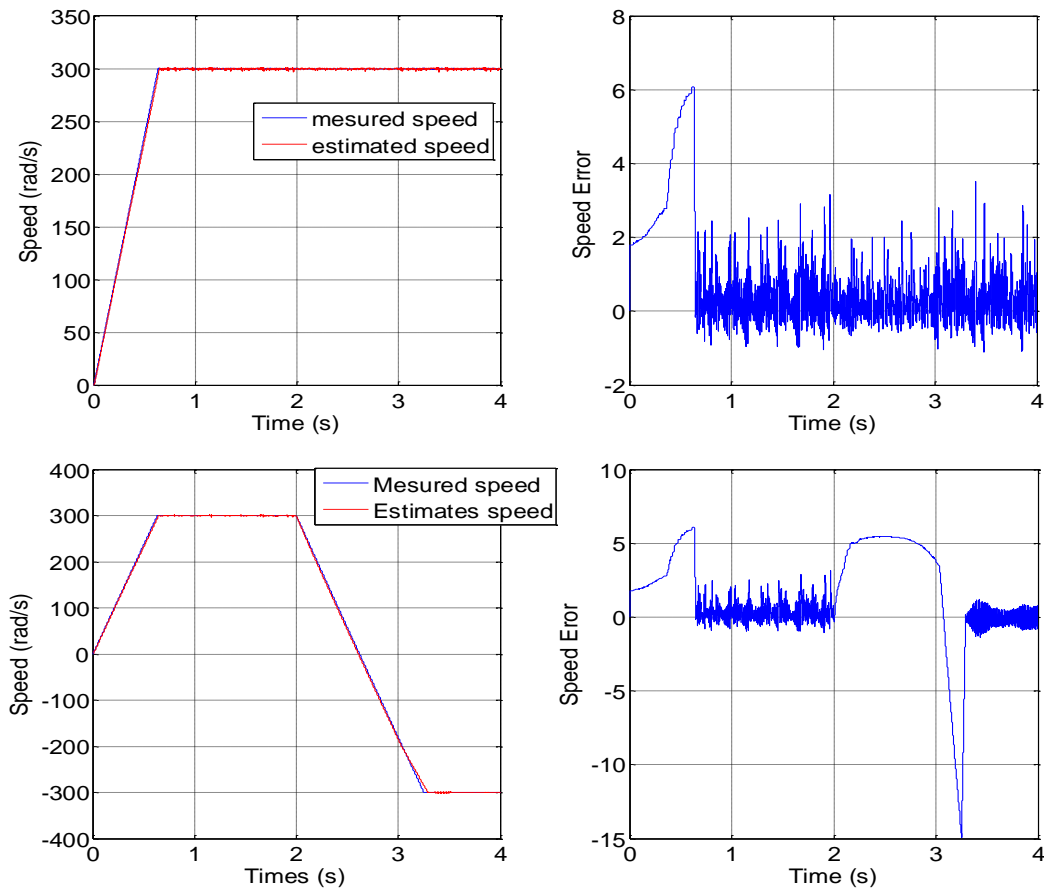


Fig. 9 The response of the observer in different speed ranges

VIII. CONCLUSION

The work we have presented has contributed to the analysis and synthesis of a robust control applied to the Dual Star Induction Machine without mechanical sensor.

The use of sliding mode, in DTC control, is a powerful tool in achieving robust and reliable control. The control with sensors was achieved using DTC control and sliding mode for the design of the speed regulator.

In this paper, an observer of speed is designed, based on MRAS techniques. The use of this observer gives results close to that obtained with using speed sensor.

With sliding mode technique, DTC controller and MRAS observer we have reached high performances in control and estimation.

REFERENCES

- [1] D. Hadiouche, "Contribution à l'étude de la machine asynchrone double étoile, modélisation, Alimentation et structure", Thèse de doctorat, Université Henri Poincaré, Nancy, France, 2001.
- [2] L.Benalia, "Commande en tension des moteurs a induction double alimentés", Thèse de doctorat, Université de Batna, Algérie 2010.
- [3] H.Ben Azza, M. Jemli, M. Boussak, M. Gossa, " High Performance Sensorless Speed Vector Control of SPIM Drives with On-Line Stator Resistance Estimation". *Simulation Modelling Practice and Theory*, Vol. 19, 2011, pp. 271-282.
- [4] K. MAROUANI, F. KHOUCHA, A. KHELOUIL, L. BAGHLI, and D. HADIOUCHE, "Study and simulation of direct torque control of double star induction motor drive", *IEEE International Power Electronics and Motion Control Conference*, May 2010, pp. 1233-1238.
- [5] R.sadouni, "Commande directe du couple (DTC-SVM) d'une MASDE associée à Deux Onduleurs Multiniveaux en Cascade avec un Redresseur à MLI Piloté par DPC", Thèse de Doctorat de l'université de Sidi Bel Abbes, Algérie, 2017
- [6] Zaimeddine R (2007), "Contrôle Direct du Couple d'une Machine Asynchrone Alimentée par de Onduleurs Multi-niveaux", Thèse de Doctorat de l'école nationale polytechnique d'Alger, Algérie, juillet (2007).

- [7] A. MARTINS, Contrôle direct du couple d'une machine asynchrone alimentée par convertisseur multiniveaux à fréquence imposée, Thèse de Doctorat de l'institut national polytechnique de Toulouse, France, Décembre 2000.
- [8] M.Abelkader, M.Sara, B. Abderrahim, W. Patrice, B.Fatima Zohra ,M. Ahmed Double star induction motor direct control with fuzzy sliding mode speed controller, *Rev. Roum. Sci. Techn. –Électrotechn. et Énerg.*, 61, 1, pp. 26–35, (2017).
- [9] A. Maasoum, A. Meroufel, A. Bentaallah, " Sliding Mode Speed Controller for a Vector Controlled Double Star Induction Motor", *Przeglad elektrotechniczny* , ISSN. 88 NR 3b/2012.
- [10] K.Kendouci, Contribution à la commande sans capteur mécanique d'une machine synchrone à aimants permanents, Thèse de doctorat, Université Mohamed Boudiaf, Oran, Algerie 2012.
- [11] I. Rouh, "Contribution à la commande sans capteur de la machine asynchrone", Thèse de Doctorat, Université de Henri Poincaré, Nancy, France, 2004.
- [12] S. Maiti, C. Chakraborty, Y.Hori, M.C. Ta, Model Reference Adaptive Controller-Based Rotor Resistance and Speed Estimation Techniques for Vector Controlled Induction Motor Drive utilizing Reactive Power, *IEEE Transactions on Industrial Electronics* Vol. 55 No. 2 (2008), 594-601
- [13] S. Maiti, C. Chakraborty, Y.Hori, M.C. Ta, Model Reference Adaptive Controller-Based Rotor Resistance and Speed Estimation Techniques for Vector Controlled Induction Motor Drive utilizing Reactive Power, *IEEE Transactions on Industrial Electronics* Vol. 55 No. 2 (2008), 594-601